Springer

KSME

Journal of Mechanical Science and Technology 30 (2) (2016) 889~902
www.springerlink.com/content/1738-494x(Print)/1976-3824(Online)
DOI 10.1007/s12206-016-0143-4

Numerical study of a water distillation system using solar energy †

K. Zarzoum[1], K. Zhani[1] and H. Ben Bacha[2,*]

[1]*LASEM (Electromechanical Systems Laboratory), National Engineering School of Sfax, B.P. W3038, Sfax University, Tunisia*
[2]*College of Engineering at Alkharj, Mechanical Engineering Department, Prince Sattam Bin Abdulaziz University, P.O.Box 655, Alkharj 11942, Kingdom of Saudi Arabia*

(Manuscript Received January 21, 2015; Revised September 17, 2015; Accepted October 23, 2015)

Abstract

This paper tackles an optimization approach in order to boost the fresh water production of a new design of a solar still which is located at Sfax engineering national school in Tunisia. This optimization approach is based upon the above mentioned design's improvement by coupling the conventional solar still into at a condenser, solar air and water collector and humidifier. This new concept of a distiller solar still using humidification- dehumidification processes (HD) is exploited for the desalination purpose. As a result of this work, the humidification- dehumidification processes have an essential effect in improving the solar still performance. Performance has been predicted theoretically in terms of water and inner glass cover temperatures, the inlet temperature of air and water of the new concept of distiller on water condensation rate and fresh water production. A general model based on heat and mass transfers in each component of the unit has been developed in steady dynamic regime. The developed model is used, simulating the HD system, to investigate the influence of the meteorological and operating parameters on the system productivity. The obtained set of ordinary differential equations has been converted to a set of algebraic system of equations by the functional approximation method of orthogonal collocation. The developed model is used to simulate the HD system in order to investigate the steady state behavior of each component of the unit and the entire system exposed to a variation of the entrance parameters and meteorological conditions. The obtained results were compared with those of other studies and the comparison gives a good validity of the present results.

Keywords: Condenser; Desalination; Dehumidification; Humidification; Solar still

1. Introduction

The availability of safe drinking water is becoming an increasingly important issue. Expanding populations, enhanced living standards and decreased availability of fresh water has catalyzed much research in the area of obtaining potable water. Since a large majority of the earth's water supply is salt water, desalination methods such as reserve osmosis and electro dialysis have been developed. In addition to the practical limitation of small- scale usage, these methods are energy demanding, costly for small amounts of fresh water require high maintenance due to the practical difficulties associated with the high operating temperature, like corrosion and scale formation and are generally coupled to fossil-fuel sources which have a negative impact on the environment. A potentially feasible alternative is solar powred desalination with a humidification - dehumidification principle. Solar energy is free, abundant and an environmentally friendly energy source. Combining the principle of humidification - dehumidification with solar desalination leads to an increase on the overall efficiency of the desalination system and therofore appears to be the best method of water desalination with solar energy despite the highest capital cost of solar energy [1]. A review of the vast literature available on solar distillation systems have revealed many observations about the design, performance and the limitation of fresh water production of solar distillation systems. A solar still output might be affected by many factors including brine depth, vapor leakage, thermal insulation, cover slope, shape material, and climate [2]. Solar stills have been extensively studied with detailed revision [3]. Thus, According to literature review, there are many investigators who have developed and studied various solar still systems, like : solar stills coupled with heat recycling [4], solar still configuration and color [5] multi-stage/multi-effect solar stills, solar stills coupled to a heat storage and hybrid solar still coupled to photovoltaic thermal systems [6]. Velmurugan et al. [7] improved the productivity of the solar still by using stepped solar still with two different depth of trays. The basin plate contains 25 trays with 10 and 18 mm depths. Integrating small fins in basin plate and adding sponges in the trays were exploited to improve the productivity. Velmurugan et al. [8] studied add-

*Corresponding author. Tel.: +966 5 06 67 84 08
E-mail address: habibbenbacha@yahoo.fr
† Recommended by Associate Editor Chang Yong Park

ing the fin at the basin solar air heater with the stepped solar still, and two different depths of trays were used. They noted that, the production of fresh water increases by 53.3% by using fins in the stepped solar still. Also, El-Sebaii et al. [9] developed a new mathematical model under the simplifying assumptions to study the thermal performance of a single basin solar still with Phase change material (PCM). El-Zahaby et al. [10] developed a new design of a stepped solar desalination system with flashing chamber to improve the fresh water productivity. The performance of stepwise water basin coupled with a spray water system by augmenting desalination productivity through using two air heaters was studied. The results showed that, the productivity and performance of the system is significantly positive dependent on both inlet sea water temperature and the power consumed. Farsad and Behzadmehr [11] solved numerically the solar desalination unit with humidification dehumidification cycle to analyze cycle parameters and to determine the amount of fresh water production. It is found that the mass flow rate, temperature of feed water, total heat flux and inlet air as well as the condenser characteristic parameter have significant effects on the cycle performance. Karan et al. [12] applied nonlinear programming techniques to optimize humidification dehumidification desalination cycles for operating conditions that result in maximum gained output ratio. Closed air open water as well as open air open water cycles, each with either an air or a water heater, were considered in this analysis. The results showed that, the GOR of all cycles was found to decrease with increasing component Terminal temperature difference (TTD). The Gained output ratio (GOR) and recover y ratio (RR) of closed air water heated Humidification dehumidification (HD) cycles were analyzed, both with zero extractions and a single extraction was studied by Ronan et al. [13]. The results showed that, the (GOR) increases and (RR) decreases as the temperature range of the cycle decreases, as the feed temperature increases or the top air temperature decreases. Juan [14] developed a new humidification and dehumidification system. In this system, the air worked in a closed loop and the evaporator prepared of treated cellulose paper substratum. This system is designed to improve the heat recovery at the condenser. Morteza et al. [15] designed and optimized a direct contact humidification- dehumidification desalination unit. From the above review, the studies dealing with stepped solar still using humidificationdehumidification systems are very few, therefore, the objective of the present work is to study the performance of the new concept of the solar still with HD processes. Bacha et al. and Zarzoum et al. [16, 17] designed a new solar still with an energy storing material, where in the basin, a flat plate solar collector and a separate condenser that coupled with the solar still were used to increase the daily productivity by increasing the temperature of the water during the day and to store the excess hot water that would extend water desalination beyond sunset.

To ameliorate the production of the solar still, we have added to this latter:

- A flat plate solar collector to increase the temperature gradient between the water and the glass cover.
- Material energy storage in the basin distiller to extend the operation of the distiller at night through the storage of excess energy.
- A pulverizer and a packed bed to increase the exchange surface and the residence time of air and water inside the solar still to increase the heat and mass transfer, and thereafter improve the production of freshwater system to increase the water temperature and the area of water in contact with the air which can accelerate the rate of evaporation.
- A plane air solar collector.
- A separate condenser for the solar distiller where condensation is produced at a temperature below that of the glass cover. The objective of this work is to:
- Establish the global model of the unit by modeling each component of the unit independently. Therefore, models, simple solar distillers, as well as air and water solar collector, humidifier (packed bed), and condenser will be respectively presented in this work. Follow the dynamic behavior of the output parameters of these two components of the unit based on its inputs and external disturbances.

2. System description

Fig. 1 shows a two-dimensional simplified schematization of the water desalination unit by solar energy. The desalination process of the installation proposed uses the humidification and dehumidification principle. Energy collection is performed by means of the solar collector and of the solar distiller. The operating principle of this system is as follows: the brackish water or the cold sea water returning in the condensation stage undergoes preheating by the latent heat of condensation. Then, water will be heated in a solar water plan. Water will be sprayed in the form of small particles by means of atomizing nozzles with high pressure or a compressed air nozzle or a piezoelectric transducer generating ultrasound. The water vaporizes in the distiller and is injected into the condensation stage to ensure the dehumidification of the vapor obtained. By cons, in packed columns, the liquid is sprayed on the packed bed between grids. The liquid phase, which contains the absorbent, forms a film on the packing elements (wetting zone). The humidified air exiting in the distiller will be conveyed to the condensation stage, where it condenses when it comes in contact with the outer walls of the tubes that circulate cold water. The amount of the condensed air produced will be collected in a tray placed below the condensation chamber. It runs along the lower edge of the glass cover. The humidifier used in the distillation prototype to increase the exchange surface and the residence time of air and water inside the solar still to increase the heat and mass transfer, and thereafter improve the production of freshwater system.

The amount of evaporated water which is not condensed will be injected again to the solar still. The hot saturated va-

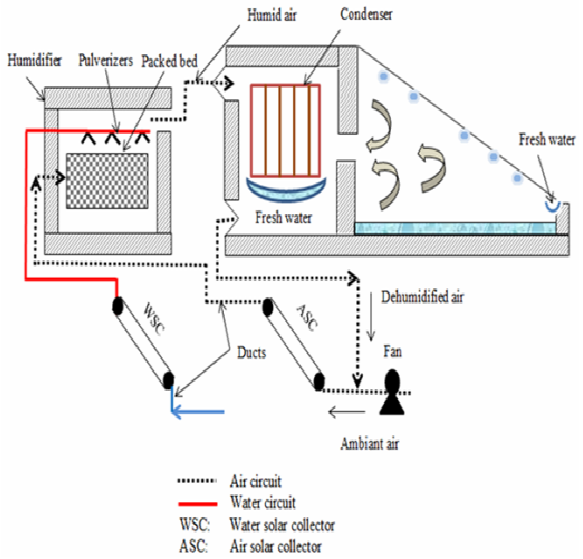

Fig. 1. Schematic view of new solar distillation system using humidification-dehumidification process.

pour coming from the solar still is driven toward the condenser where it condenses in contact with the cold plates of the condenser. The distilled water is collected in a basin at the bottom of the condensation tower. Energy collection is performed by means of the water and air solar collector and of the solar still. The flat plate water solar collector has an absorber with parallel and narrow channels. In this case, the fluid circulates in a forced convection and in one direction. The solar desalination unit consists of two water solar collectors and two air solar collectors.

3. Thermal modeling

The water desalination unit by solar energy using the principle of humidification / dehumidification can be considered as an important class of thermal processes because of the presence of phenomena heating, evaporation and condensation. It is characterized by the fact that these quantities are different depending on the space and time. So the dynamic behavior of this type of process is generally described by distributed parameter systems represented by systems of PDEs. The following section presents the dynamic modeling of the water and air solar collector, solar still with humidifier and energy storing material modeling, and the condenser. The models developed are a set of partial derivative equations, derivative equations and algebraic equation. The model is based on a number of assumptions previously described elsewhere [18-20].

3.1 Water solar collector model

The flat plate water solar collector has an absorber with parallel and narrow channels. In this case, the fluid circulates in a forced convection and in one direction.

The principal assumptions used to obtain the mathematical model under steady state regime are [8]:

- The speed of the fluid is uniform,
- The absorber and fluid have the same temperature at any point,
- The fluid temperature remains under 100°C point.

The below simulation results were obtained for the properties of the water solar collector which are: Aperture area is 2 m^2, the inner diameter of the tubes is 10 mm and the outer one is 12 mm, the effective transmission absorbtion is 0.7, the riser tubes materiel iscopper, absorber surface is paint mat black, the loss coefficient is 4.8 W/m.K Back insulation, thickness is fiber glass, 50 mm.

The energy balance equation for the system formed by the absorber and the fluid formed for a slice of the collector having a width of l, a length of dx, and a surface of ds, is expressed by the following equation:

$$\frac{\partial T_w}{\partial t}=\frac{1}{\delta}\left(-m_w\xi\frac{\partial T_w}{\partial x}-T_w+f(t)\right) \tag{1}$$

with:

$$\xi=\frac{C_w}{U_w l} \tag{2}$$

$$\delta=\frac{(MC)_g}{U_w A} \tag{3}$$

$$(MC)_g=M_w C_w+M_{ab}C_{ab} \tag{4}$$

$$f(t)=\frac{\tau_v\alpha_{ab}I(t)}{U_w}+T_{amb}(t). \tag{5}$$

3.2 Solar still with energy storing material modeling :

The dynamic mathematical model of the solar still with humidifier and energy storing material consisted of a set of equations that were developed using thermal and mass balances for the water phase, the air phase, and the air-water interface.

- Heat balance for the glass cover

$$M_v C_v dT_g=IA_v dt+h_{rwv}(T_w-T_g)dt+h_{evp}(T_w-T_g)dt$$
$$-h_{rc}(T_g-T_{amb})dt. \tag{6}$$

- Heat balance for the basin absorber

$$M_b C_b dT_b=IA_b dt-h_{cbw}(T_b-T_w)dt$$
$$-U_{loss}(T_b-T_{amb})dt. \tag{7}$$

- Heat balance for the water basin

$$(M_w C_w+M_{em}C_{em})dT_w=IA_w dt+h_{cbw}(T_b-T_w)dt$$
$$-h_{rwv}(T_w-T_g)dt-h_{cwv}(T_w-T_g)dt-h_{evp}(T_w-T_g)dt. \tag{8}$$

• The water condensation rate in solar still

$$d\dot{m} = \frac{hevp\left(T_w - T_g\right)3600}{L} \tag{9}$$

where the evaporation coefficient of the basin to the glass cover:

$$h_{evp} = 16 \cdot 273\left(10^{-3}\right)h_{cwv}\frac{\left(P_w - P_v\right)}{T_w - T_g}. \tag{10}$$

The convection coefficient of the basin cover glass:

$$h_{cwv} = 0.884\left[T_w - T_g + \frac{\left(P_w - P_v\right)\left(T_w + 273\right)}{268.9\,10^3 - P_w}\right]^{\frac{1}{3}}. \tag{11}$$

The coefficient of heat transfer by convection between the basin and the water:

$$h_{cbw} = 135\ W/m^2K. \tag{12}$$

The radiation coefficient from the water to the glass:

$$h_{rwv} = \varepsilon_{eff}\sigma\frac{\left[\left(T_w + 273\right)^4 - \left(T_g + 273\right)^4\right]}{T_w - T_g} \tag{13}$$

$$\varepsilon_{eff} = \left[\frac{1}{\varepsilon_w} + \frac{1}{\varepsilon_v} - 1\right]^{-1}. \tag{14}$$

The coefficient of convective radiative heat transfer in the solar distiller from glass cover to the ambient air:

$$h_{cr} = h_{cva} + h_{rva} \tag{15}$$

$$h_{rva} = \varepsilon_v\sigma\frac{\left[\left(T_g + 273\right)^4 - \left(T_{amb} + 273\right)^4\right]}{T_g - T_{amb}} \tag{16}$$

$$h_{cva} = 5.7 + 3.8V_{wind}. \tag{17}$$

3.3 Humidifier modeling (The packed bed)

• Heat and mass balance at the packed bed:

To develop a mathematical model that describes accurately the behavior of distiller (at packing), we motto the latter in volume elements of length dx and apply in second place the balances of heat and mass transfer on the volume element we choose. The formulation of the mathematical model based on heat and mass balances can determine the coupling equations between the water temperature, the air temperature and the water content of the moist air in the packed bed. The below simulation results were obtained for the properties of the humidifier which are:

Size: 0.5 x 0.5 x 0.7m^3

Packed bed: Cellulosic materiel

- Water phase: [Amount of energy stored in the volume element of height dz] = [(amount of heat carried away by the water during dt) - (amount of heat transmitted to the interface water-air during the same time interval dt)].

The heat balance of water in a volume element of packed bed with height dz and during time interval dt is given by the following equation:

Mathematically this can be expressed as:

$$M_wC_{pw}dT_ldz = m_wC_{pw}dT_ldt - U_w\left(T_i - T_l\right)dzdt. \tag{18}$$

It can be further simplified as:

$$\frac{dT_l}{dt} = \frac{1}{M_wC_{pw}}\left(m_wC_{pw}\frac{dT_l}{dz} - U_w\left(T_i - T_w\right)\right). \tag{19}$$

- Air phase: [Amount of energy accumulated in the volume element of length dz] = [(amount of heat received by the interface water-air during the interval of time dt) - (Quantity of heat transmitted to the flow of air during the same time dt)].

The heat balance of air in a volume element of packed bed with length dz and during time interval dt is given by the following equation: Mathematically this can be expressed as:

$$M_aC_{pa}dT_adz = U_a\left(T_i - T_a\right)dzdt - m_aC_{pa}dT_adt. \tag{20}$$

It can be further simplified as:

$$\frac{dT_a}{dt} = \frac{1}{M_aC_{pa}}\left(U_a\left(T_i - T_a\right) - m_aC_{pa}\frac{dT_a}{dz}\right). \tag{21}$$

- Air-water interface : [Amount of heat transmitted from the water current through the liquid film to the surface of the water-air separation] = [(amount of heat transmitted from the surface separation through the film gas to the gaseous stream) + (Quantity of heat applied to evaporate the amount of water transferred from the mass of liquid through the interface to the gas stream)].

At the air-water interface, heat balance can be written in the following form:

$$U_w\left(T_i - T_l\right) = U_a\left(T_i - T_a\right) + \lambda_oU_m\left(W_i - W_a\right). \tag{22}$$

The mass balance at the air-water interface is given by the following equation:

$$\frac{dW_a}{dt} = \frac{1}{M_a}\left(U_m\left(W_i - W_a\right) - m_a\frac{dW_a}{dz}\right). \tag{23}$$

To be numerically integrated, the above equations are com-

pleted with both empirical correlations of the voluminal heat coefficients (Uw,Ua) and mass transfer coefficient (Um) which are obtained by Amara et al. [21] and an algebraic equation of the curve of saturation of water steam [22]

$$U_m = 0.6119 * m_w^{0.1002} * m_a^{0.3753} * zl^{-0.0986} \quad (24)$$

$$U_w = 25223.5 * m_w^{0.0591} m_a^{0.1644} * zl^{-0.0542} . \quad (25)$$

The air-film heat transfer coefficient and the mass transfer coefficient on the air-water interface are coupled by the Lewis relation as follows:

$$U_a = C_{pa} U_m . \quad (26)$$

Stoecker and Jones [23] suggest that the system of equations developed and an additional equation of the absolute humidity of the air will be used to monitor the variation of different parameters at any point in the distiller.

The curve of saturation of water steam is given by the following equation:

$$W_i = 0.62198 \frac{P_i}{1 - P_i} \quad (27)$$

where Pi denotes the partial pressure of water vapor to the dry bulb temperature (atm) , it is given by the following relationship:

$$P_i = \varphi P_{WS} \quad (28)$$

where φ and Pws are respectively the relative humidity and the saturation pressure of water vapor in the air to the dry bulb temperature (atm).

The saturation partial pressure of water vapor in the air is given by the empirical relationship simplified Keenan Kyes. This relation is valid for temperatures between 10 and 150°C. Where,

$$\log\left(\frac{P_{ws}}{218{,}167}\right) = -\frac{\beta}{T_i}\left(\frac{a + b\beta + c\beta^2}{1 + d\beta}\right) \quad (29)$$

$$\begin{aligned} \beta &= 647.27 - T_i \\ a &= 3.2437814 \\ b &= 5.86823\,10^{-3} \\ c &= 1.1702379\,10^{-8} \\ d &= 2.18\,78462\,10^{-3} . \end{aligned} \quad (30)$$

3.4 Air solar collector modeling

The plane air solar collector consists of an absorber shaped like of rectangular parallel channels in copper, a glass cover and insulation. For the air solar collector, the model is based on Nafey's work [24]. The assumptions used in developing the model are listed below:

- The coefficient of exchange of the copper is very high, so we can suppose that the absorber is a flat plate,
- The velocity of air is uniform, therefore the local state of air depends only on one side x,
- The cross-section area of the absorber, glass cover and air are equal.

The below simulation results were obtained for the properties of the air solar collector which are: Aperture area = 2 m^2 absorber plate material is copper, absorptivity of plate is 0.9, the absorptivity of glass cover is 0.1, the back insulation, the thickness is polyurethane, 20 mm, the emissivity of plate is 0.94, the emissivity of glass cover is 0.987 and the transmissivity of glass cover is 0.875.

For the absorber plate element,

$$\frac{\partial T_{pl}}{\partial t} = \frac{A}{M_{pl} C_{pl}} \begin{bmatrix} I \tau_v \alpha_{pl} - U_{loss}\left(T_{pl} - T_{amb}\right) - hco_{pl-a}\left(T_{pl} - T_a\right) \\ -hrad_{pl-v}\left(T_{pl} - T_v\right) \end{bmatrix} . \quad (31)$$

For an air element,

$$\frac{\partial T_a}{\partial t} = \frac{A}{M_a C_a}\left[hco_{pl-a}\left(T_{pl} - T_a\right) + hco_{v-a}\left(T_v - T_a\right)\right] - \frac{Am_a}{bM_a}\frac{\partial T_a}{\partial x} . \quad (32)$$

For the glass cover element

$$\frac{\partial T_v}{\partial t} = \frac{A}{M_v C_v} \begin{bmatrix} I \alpha_v + hrad_{pl-v}\left(T_{pl} - T_v\right) - hco_{v-a}\left(T_v - T_a\right) \\ -hcr_{v-amb}\left(T_v - T_{amb}\right) \end{bmatrix} . \quad (33)$$

3.5 Condenser modeling

The dynamic mathematical formulation for the condensation tower was developed using thermal and mass balances. This formulation gave the coupling equations that relate temperature, the temperature of the cooling water, and the absolute humidity of the humid air. The balances were applied to an element of volume of the condensation tower having a height dz. Three key parameters of air are considered in the parametric study of the condensation tower. These are humidity of air at the entrance of the condensation tower (We), air flow rate (mgt) and the air temperature at the entrance of the condensation tower of the solar still (Tgc).

Water phase

$$M_f C_f dT_f dz = U_f A_c \left(T_{ic} - T_f\right) dzdt - D_f C_f dT_f dt \quad (34)$$

$$\frac{\partial T_f}{\partial t} = -\frac{D_f}{M_f}\frac{\partial T_f}{\partial z} + \frac{UA_c}{M_f C_f}\left(T_{ic} - T_f\right) . \quad (35)$$

Air phase

$$M_g C_{pg} dT_g dz = m_g C_{pg} dT_g dt - U_g A_c \left(T_g - T_{ic}\right) dzdt - \lambda_o U_{mc} A_c \left(W_g - W_{ic}\right) dzdt. \quad (36)$$

Air-condensate interface

The heat balance at air-condensate interface is given by the following equation:

$$U_g A_c \left(T_g - T_{ic}\right) + U_f A_c \left(T_{ic} - T_f\right) = \lambda_o U_{mc} A_c \left(W_g - W_{ic}\right). \quad (37)$$

The mass balance at air-condensate interface is given by the following equation:

$$M_g dW_g dz = m_g dW_g dt + U_{mc} A_c \left(W_g - W_{ic}\right) dzdt. \quad (38)$$

The water condensation rate was determined using the following algebraic equation that relates the variation of water content to the height of the tower:

$$dm_c = K_{mc} A_c \left(W_{ic} - W_{gc}\right) dz \quad (39)$$

$$\frac{1}{U_f} = \frac{1}{h_e\left(\frac{d_e}{d_i}\right)} + \frac{1}{h_c} + R_{ee}\left(\frac{d_e}{d_i}\right) + R_{ec} + \frac{d_e}{2\lambda_p} Log\left(\frac{d_e}{d_i}\right) \quad (40)$$

$$h_e = \frac{\lambda_e}{d_i} 0.023 R_e^{0.8} \Pr^{0.4} \quad (41)$$

$$h_c = 0.943\left(\frac{g\rho_c^2 \lambda_c^3 \lambda_o}{L\mu_c\left(T_i - T_p\right)}\right)^{\frac{1}{4}} \quad (42)$$

$$U_g = \frac{\lambda_g}{d_e} 1.04 \mathrm{Re}^{0.4} \Pr^{0.36} \quad (43)$$

$$U_{mc} = \frac{U_g}{C_{pg}} \quad (44)$$

$$W_{ic} = 0.62198 \frac{P_{ic}}{1 - P_{ic}}. \quad (45)$$

4. Approximation of mathematical models

The analytical solution of equations of global mathematical model is impossible and they must be discretized to obtain approximate, but still accurate, solutions. The method of finite differences has been used quite extensively in the past, but it usually requires a large number of discretization points and results in a correspondingly large set of Ordinary differential equations (ODE). On the other hand, the Orthogonal collocation method (OCM) approximates the solution by a polynomial trial function, and the resulting set of ODE is often considerably smaller. Currently, the collocation method is very widely used in chemical and biotechnological engineering problems [25, 26].

4.1 Formulation of the approximation method

Consider the following Partial differential equation (PDE): Formulation of the approximation method: Consider the following Partial differential equation (PDE): To study a collocation method in this model, the following approximation series is used for the variable T:

$$\frac{\partial T}{\partial t} = f\left(x, t, \frac{\partial T}{\partial x}, ...\right). \quad (46)$$

With

$t \in T = [0, t_f]$: Time domain $t_f < \infty$.

$x \in T = [x_0, x_1]$: Spatial domain.

To study a collocation method in this model, the following approximation series is used for the variable T:

$$\overline{T}(x,t) = \sum_{i=1}^{N} \chi_i(t) \varphi_i(x). \quad (47)$$

The specific method applied is called orthogonal collocation due to certain orthogonality properties of the base functions φ. Due to technical reasons, the number of the base functions is given in the form of N +2. The points x0, and x, correspond to the initial and end points of the system. Consequently, the number of internal collocation points is N.

By using the Lagrange interpolation polynomial, as a base Lj function, the Eq. (38) can be written as follows:

$$\overline{T}(x,t) = \sum_{j=0}^{N+1} L_j(x) T_j(t) \quad (48)$$

$$\text{With,} \qquad L_j(x) = \prod_{i=0}^{N+1} \left(\frac{x - x_i}{x_j - x_i}\right) \quad (49)$$

$$T_j(t) = \overline{T}(x = x_j, t). \quad (50)$$

Xj, (j = 0,1,……N+1) : the collocation points. With this method, the derivatives with respect to time and space are approximated as follows:

$$\frac{\partial \overline{T}(x,t)}{\partial t} = \sum_{j=0}^{N+1} L_j(x) \frac{dT_j(t)}{dt} \quad (51)$$

$$\frac{\partial \overline{T}(x,t)}{\partial x} = \sum_{j=0}^{N+1} \frac{dL_j(x)}{dx}(t). \quad (52)$$

At the different collocation points, we can write:

$$\left.\frac{\partial \overline{T}(x,t)}{\partial t}\right|_{x=x_i} = \frac{dT_i(t)}{dt} \quad (53)$$

$$\left.\frac{\partial \overline{T}(x,t)}{\partial t}\right|_{x=x_i} = \sum_{j=0}^{N+1} l_{ij} T_j(t) \quad (54)$$

$$\text{With,} \quad l_{ij} = \left.\frac{dL_j(x)}{dx}\right|_{x=x_i}. \quad (55)$$

4.2 Formulation of the approximation method

By substituting the approximations presented earlier in the initial system formed by partial derivatives equations, we can get a system of ordinary differential equations according to the time localized in every collocation point.

• Water solar collector reduced dynamic model:

$$\frac{dT_{wi}}{dt}=\frac{1}{\delta}\left(\left(-m_w\xi\right)\left(\sum_{j=1}^{N+1}l_{ij}T_{wj}+l_{0j}T_{we}\right)-T_{wi}+f\left(t\right)\right). \tag{56}$$

• Air solar collector reduced dynamic model:

$$\frac{dT_{vi}}{dt}=\frac{A}{M_vC_v}\begin{bmatrix}I\alpha_v+hrad_{pl-v}\left(T_{pli}-T_{vi}\right)-hco_{v-a}\left(T_{vi}-T_{ai}\right)\\-hcr_{v-amb}\left(T_{vi}-T_{amb}\right)\end{bmatrix} \tag{57}$$

$$\frac{dT_{pli}}{dt}=\frac{A}{M_{pl}C_{pl}}\begin{bmatrix}I\tau_v\alpha_{pl}-U_{loss}\left(T_{pli}-T_{amb}\right)-hco_{pl-a}\left(T_{pli}-T_{ai}\right)-\\hrad_{pl-v}\left(T_{pli}-T_{vi}\right)\end{bmatrix} \tag{58}$$

$$\frac{dT_{ai}}{dt}=\frac{A}{M_aC_a}\left[hco_{pl-a}\left(T_{pli}-T_{ai}\right)+hco_{v-a}\left(T_{vi}-T_{ai}\right)\right]-\frac{Am_a}{bM_a}\left[\sum_{j=1}^{N+1}l_{ij}T_{aj}+l_{i0}T_{a0}\right]. \tag{59}$$

• Solar still reduced dynamic model:

$$\frac{dT_{vi}}{dt}=\frac{1}{M_vC_v}\left(IA_v+h_{rwv}\left(T_{wi}-T_{vi}\right)+h_{evp}\left(T_{wi}-T_{vi}\right)-h_{rc}\left(T_{vi}-T_{amb}\right)\right) \tag{60}$$

$$\frac{dT_{bi}}{dt}=\frac{1}{M_bC_b}\left(IA_b-h_{cbw}\left(T_{bi}-T_{wi}\right)-U_{loss}\left(T_{bi}-T_{amb}\right)\right) \tag{61}$$

$$\frac{dT_{wi}}{dt}=\frac{1}{\left(M_wC_w+M_{em}C_{em}\right)}\begin{pmatrix}IA_w+h_{cbw}\left(T_{bi}-T_{wi}\right)-h_{rwv}\left(T_{wi}-T_{vi}\right)-\\h_{cwv}\left(T_{wi}-T_{vi}\right)-h_{evp}\left(T_{wi}-T_{vi}\right)\end{pmatrix}. \tag{62}$$

• Humidifier reduced dynamic model:

$$\frac{dT_{Li}}{dt}=\frac{1}{M_wC_{pw}}\left[m_wC_{pw}\left(\sum_{j=0}^{N}l_{ij}T_{Lj}+l_{iN+1}T_{L2}\right)\right] -U_w\left(T_i-T_{Li}\right) \tag{63}$$

$$\frac{dT_{ai}}{dt}=\frac{1}{M_aC_{pa}}\left[U_a\left(T_i-T_{ai}\right)\right] -m_aC_{pa}\left[\sum_{j=1}^{N+1}l_{ij}T_{aj}+l_{i0}T_{a0}\right] \tag{64}$$

$$\frac{dW_{ai}}{dt}=\frac{1}{M_a}\left(U_m\left(W_i-W_{ai}\right)-m_a\left[\sum_{j=1}^{N+1}l_{ij}W_{aj}+l_{i0}W_{a0}\right]\right) \tag{65}$$

$$U_w\left(T_i-T_{li}\right)=U_a\left(T_i-T_{ai}\right)+\lambda_oU_m\left(W_i-W_{ai}\right) \tag{66}$$

$$W_i=0.62198\frac{P_i}{1-P_i}. \tag{67}$$

• Condenser reduced dynamic model

$$\frac{dT_{fi}}{dt}=-\frac{D_f}{M_f}\left[\sum_{j=1}^{N+1}l_{ij}T_{fi}+l_{i0}T_{f1}\right]+\frac{U_fA_c}{M_fC_f}\left(T_{Ic}-T_{fi}\right) \tag{68}$$

$$\frac{dT_{gci}}{dt}=\frac{m_{gt}}{M_{gc}}\left[\sum_{j=0}^{N}l_{ij}T_{gci}+l_{iN+1}T_{gc2}\right]-\frac{h_{gc}A_c}{M_{gc}C_{gc}}\left(T_{gci}-T_{Ic}\right) -\frac{\lambda_oK_{mc}A_c}{M_{gc}C_{gc}}\left(W_{gci}-W_{Ic}\right) \tag{69}$$

$$\frac{dW_{gci}}{dt}=\frac{m_{gt}}{M_{gc}}\left[\sum_{j=0}^{N}l_{ij}W_{gci}+l_{iN+1}W_{gc2}\right]+\frac{K_{mc}A_c}{M_{gc}}\left(W_{gci}-W_{Ic}\right) \tag{70}$$

$$h_{gc}A_c\left(T_{gci}-T_{Ic}\right)+UA_c\left(T_{Ic}-T_{ei}\right)=\lambda_oK_{mc}A_c\left(W_{gci}-W_{Ic}\right) \tag{71}$$

$$W_{Ic}=0.62198\frac{P_{Ic}}{1-P_{Ic}}. \tag{72}$$

5. Simulation and results discussion

5.1 Numerical simulation in dynamic regime of solar still

The set of equations presented above is used to determine the outlet parameters (air temperature, water temperature, glass temperature, absorber temperate the effect of the humidity on fresh water production and the fresh water condensate) of each component of the desalination unit while guessing the inlet of the same parameters. For this purpose, the set of ordinary differential equations is converted to a set of algebraic equations by a functional approximation technique: the orthogonal collocation. The numerical simulation allows the understanding and the characterization of the steady state behavior of each component of the unit. A numerical computer program is developed using the Borland C++ software to solve the mathematical models. In order to evaluate the performance of the regenerative solar distiller, simulations were conducted. In Fig. 2, it can be seen that for the modified still, the water and absorber temperatures are higher than the glass cover temperatures in the function of time throughout the day, except in the evening, which is also due to the higher thermal capacity of the basin water mass. The curves increase gradually at the beginning of the day, reaching a maximum between 12h and 14h, then decrease gradually. It is also observed that the water temperature and the absorber (pelvis) are almost the same because of the contact with the last two heat transfer by convection directly. The temperature of the absorber reaches a maximum value of 85°C; this is explained by the relatively high absorption coefficient of black paint. It was noticed that the water and absorber outlet temperature exactly follow the behaviour of the solar radiation. On the other hand, all the temperatures showed similar trends of increasing with the respective increasing of solar radiation of respective during the day. These results indicate that solar radiation has a greater influence on the thermal performance of the solar still. Bilal et al. [27] and Murugavela et al. [28] found that the technique of adding the absorbent black material that is used in the basin with water (can store more amount of heat energy to increase

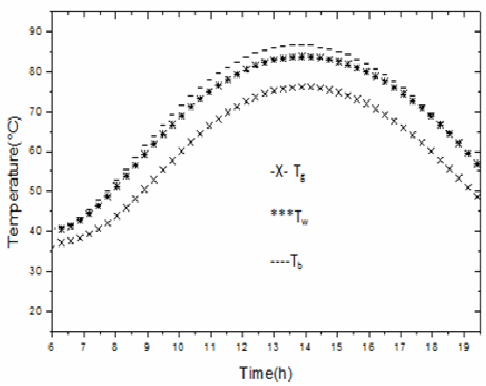

Fig. 2. Hourly variations of different temperatures.

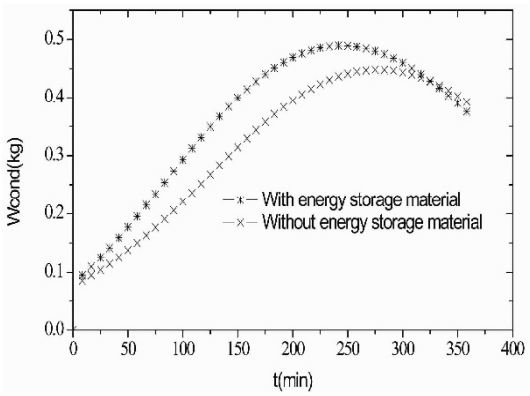

Fig. 3. Effect of the energy storage materials on the distillate water in function of time (Energy storage material: cement).

the heat capacity of the basin and to increase the production night as quartzite, pieces of red bricks, pieces of concrete cement, lime stones and pieces of iron ... etc..) In this section, we have studied the effect of material energy storage taking into account that the distiller is coupled with a preheating system (solar water collector).

For this study, we have used, as a heat storage material, sensitive pieces of cement concrete. The hourly production of distilled water for two types of distillers is shown in Fig. 3. This production begins to be significant from 100 min of sunshine. We note that the distiller contains material energy storage that has the largest production that the distiller without them. Fig. 4 shows the variation of the accumulated distillate water for a typical summer day. We note that the curve of the total production is almost zero at the beginning of the day, and then begins to rise until reaching a total amount of 8.80 kg/m^2.jour. The productions of solar distiller freshwater increases when the brine temperature rises.

5.2 Numerical simulation in dynamic regime of an air solar heater

Due to the variable nature of the meteorological conditions around the world, it is critical to note that solar thermal collectors have a variable efficiency, dependent on solar insolation, air flow rate and air temperature. The numerical investigation presented in this section consists in an evaluation of the influence of the operating and weather parameters on the air solar collector performances; outlet air temperature and thermal efficiency. The thermal efficiency of the air solar collector was defined as the ratio of the useful energy gained air after passage through the air solar collector to the total incident solar radiation. This is expressed by the following equation:

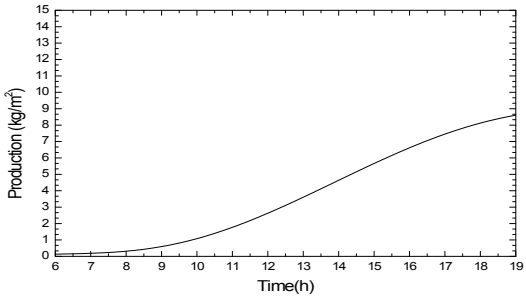

Fig. 4. Variation of the accumulated distillate water for a typical summer day.

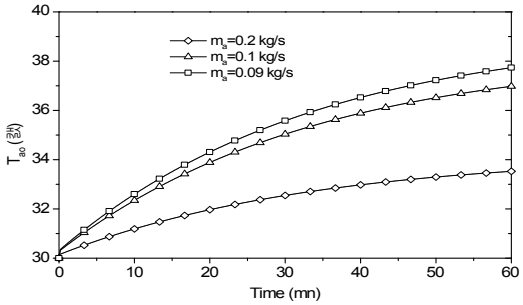

Fig. 5. Effect of solar radiation on the air collector outlet temperature as a function of time.

$$\eta = \frac{m_a C_a \left(T_{ao} - T_{ai}\right)}{S\,I} \tag{73}$$

where ma is the mass flow rate of the transpired humid air, Ca is the air heat capacity, Tao is the outlet air temperature, Tai is the inlet air temperature, I is the solar irradiation intensity and S is the air solar collector surface. Figs. 5 and 6 show the effect of solar radiation on the air collector outlet temperature as a function of time and the impact of the air flow rate on the outlet air temperature.

5.2.1 Effect of solar irradiation and air flow rate

The variation of outlet air temperature and thermal efficiency with solar irradiation and air flow rate are depicted in Fig. 5. Fig. 5 shows that the solar irradiation has a similar effect on the collector thermal performance. In fact, increasing the solar insolation increases the outlet air temperature and the thermal efficiency.

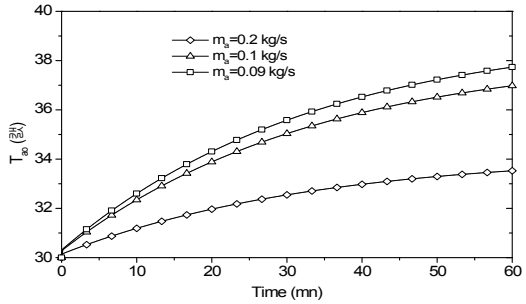

Fig. 6. Impact of the air flow rate on the outlet air temperature. Tae = 30°C, Tamb = 15°C, Tve = 30°C, Tple = 32°C and I = 800 W/m^2.

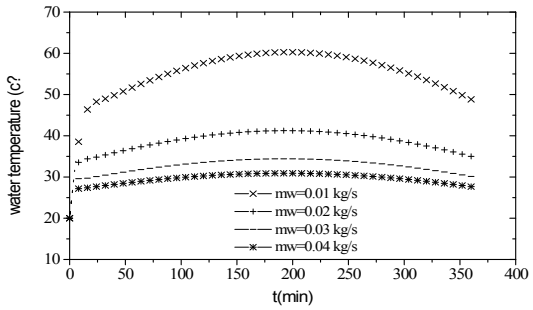

Fig. 7. Evolution of the water temperature at the outlet in function of time Tamb = 20°C, Twe = 20°C for different water flow.

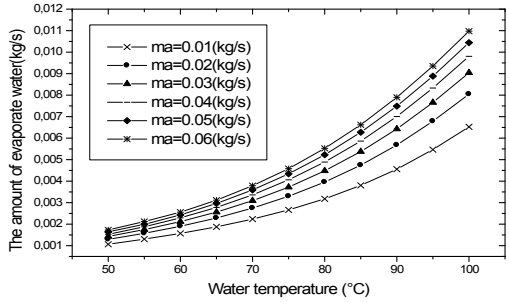

Fig. 8. Evolution of amount of evaporate water in function of water temperature and air flow rate.

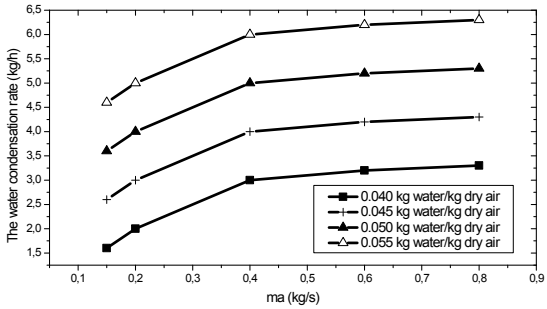

Fig. 9. Effect of air flow rate and specific humidity at the inlet of condenser on the water condensation rate.

5.2.2 Impact of the air flow rate on the outlet air temperature

In contrary, the air flow rate has an antagonist impact on thermal performance of the solar collector as shown in Fig. 6. From Fig. 6, it can be seen that the outlet air temperature is strongly dependent on the air flow rate. The outlet air temperature decreases with an increase of air flow rate.

5.3 Numerical simulation of water solar collector

The numerical simulation in a dynamic regime of the behavior of solar water is used to find the influence of the mass flow of water (mw) below the outlet temperature of the water (Tw). Fig. 7 shows the influence of water flow on the variation of the water temperature at the outlet of the solar collector to the operating conditions. This figure shows that the water temperature at the outlet of the sensor decreases when increasing the flow rate of the water flowing through the solar collector water.

5.4 Numerical simulation in dynamic regime of the humidifier

Fig. 8 represents effect of air flow rate ma and water flow rate mw which varies between 0.01 and 0.06 kg/s on amount of evaporate water which will be condensed in the solar still in function of inlet temperature of water which are pulverize under the packed bed. As seen in this figure, increasing air flow rate and air humidity increases the amount of evaporate water. From this figure, it can be seen that the air humidity produced in the basin of the solar still increase with increasing of the air. Fig. 9 indicates that the water condensation rate increases meaningfully with the moist air flow rate and the absolute humidity. But it increases slightly when the moist air flow rate is in the range of 0.4-0.8 kg/s under the effect of water flow which are pulverize under the packed bed to increase the exchange surface and the residence time of air and water inside the solar still to increase the heat and mass transfer, and thereafter improve the production of freshwater system. This result implies that it exist an optimum value of moist air flow rate where the water condensation rate is maximum.

Fig. 10 shows the evolution of amount of evaporate water in function of air temperature and air flow rate which will be condensed in the solar still. The first thing that can be drawn, from this figure that follows is that the amount of evaporate water increases proportionally with increasing of air flow rate which varies between 0.01 and 0.06 kg/s. The curves vary in a progressive manner up to a certain value and then remain constant. The curves can be divided into three parts: The first part of the curves is an increasing slope is slow progression of the amount of humid air into the solar still. In this part the amount of humid air produced in the solar still have not yet sufficient to heating the medium and mass transfer and for it the production of distilled water remains low. The second part of the curves present growing right, this is the most remarkable part of the curves. The curves vary rapidly by this part this timeliness is due to the gradient of air temperature. When the air humidity increases the probability of mass transfer increases

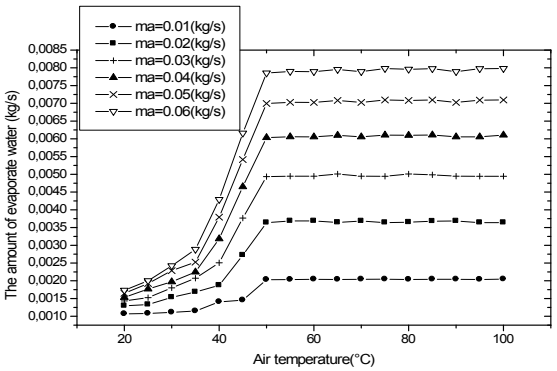

Fig. 10. Evolution of amount of evaporate water in function of air temperature and air flow rate.

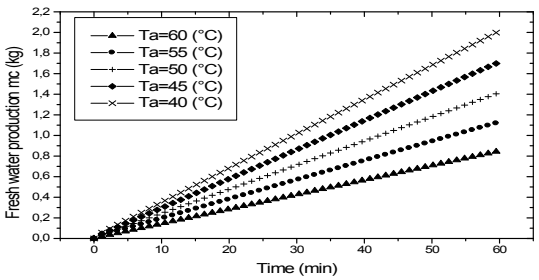

Fig. 11. Effect of the inlet temperature of air of the new concept of distiller on water condensation rate.

and the backgrounds will be more concentrated, which brings up the water droplets. Water condenses at this level through the enrichment backgrounds by moisture due in part to the temperature of hot water sprayed on the packed bed and above all the other with the heated air by through the solar air collector. The third part of the curves has the allure of a horizontal line with negligible variation. This stability is due to the concentration of vapor backgrounds. Therefore, according to these results, one can conclude that it is interesting to work with elevated air flow rate at the inlet of the solar still to increase the amount of the evaporate water which will be condensed in the solar still and to provide a better output of air humidity. The air humidity at the inlet of the solar still will be transferred to the condenser and will be condensed on the external pipe walls of the condenser. So, its value is variable. Therefore it is interesting to raise the influence of this parameter on air humidity at the solar still.

5.5 Numerical simulation in dynamic regime of the condenser

The influence of the inlet temperature of air of this new concept of distiller on water condensation rate is shown in Fig. 11. for the following operating conditions: I = 800 W/m², mw = 0.1 kg/s, ma = 0.2 kg/s Tamb = 30°C, Tw = 20°C, Ta = 50°C, Wg = 0.287 kg water/kg dry air.

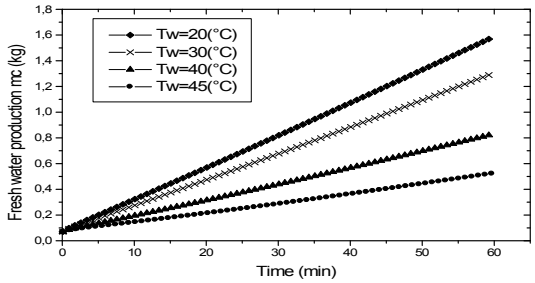

Fig. 12. Effect of the inlet temperature of air of the new concept of distiller on water condensation rate.

It is noted that the amount of condensate is sensitive to the variation of the temperature of the humid air. An increase in the air humid temperature causes a remarkable increase in water condensation rate mc. The water condensation rate increases significantly and according to the air temperature (T) at the condensation tower inlet. That is, the increase of the air temperature at the condensation tower inlet produces more heat inside it. We can conclude that it is interesting to work with high inlet temperature of humid air in the solar distiller to increase the production of distilled water.

Fig. 12 shows the influence of the temperature of water at the inlet of condenser on the water condensation rate for the following operating conditions: ma = 0.2 kg/s, mw = 0.1 kg/s, Tamb = 30°C, Ta = 50° and I = 800 W/m². It is clear that the temperature of water at the entrance of condenser has an impact on water condensation rate. In this figure, we find that an increase in the inlet temperature of the cooling water in the condenser tubes results in a reduction of the production of desalinated water. So it is advantageous to work with water cooling having a lowest possible temperature in order to allow the condensation tower to provide a better performance. For one hour of operation and to Tw1 equal to 20°C, the amount of condensate, m takes the value of the order of 1.6 kg while for a value of Tw1 equal to 45°C, the amount of condensate, m takes the value of the order of 0.57 kg. Therefore according to these values, a 55% reduction of the temperature of the cooling water produces an additional 64.37% of condensate.

The available data in Table 1 show that the production of solar still distiller coupled to a condenser, solar air and water collector and packed bed is higher than the production of other types of distillers. The following table includes the daily production of some typical distillers existing in the literature. This production is significant; it varies from 4 to 10.5 kg/m^2 .day updated throughout the year. The addition of these components to the conventional solar still has an influence on the flow of the water produced. This may be due to the humidification- dehumidification processes.

6. Conclusions

In the present study, the performance of the unit which consists of a conventional solar still coupled to a condenser, solar

Table 1. Comparison of solar stills productivity.

Type of distiller	Wind speed	Ambient temperature (°C)	Location (latitude)	Authors	Production (kg/m^2/day)
Spherical distiller	2	25-30	Alger 36.833 36° 49'N	A. Chaker and G. Menguy (2001)	4-7
A weir-type cascade solar still	0-9	25-33	Zahedan, Iran (29.5°N)	Tabrizi et al. (2010)	5.1
A solar still augmented with a flat-plate collector	–	19-30	Amman, Jordan (31.6°N)	Badran et al. (2005)	0-2.3
A passive solar still with a separate condenser	2	20-28	Glasgow, UK (55.5°N)	Madhlop and Johnstone (2009)	~6.0
A single basin double slope solar still with energy storing materials	0.2-1.2	20-27	Tamil Nadu, India (11.2°N)	Murugavel et al. (2010)	~2.1
A solar still with energy storage medium - jute cloth	–	11-22	Fukuoka, Japan (33.2°N)	Sakthivel et al. (2010)	~4.0
Distiller coupled to a condenser, solar air and water collector and packed bed	1	20-30	Sfax 34°44'26"N	Present work	4-8.5

air and water collector and packed bed stepped with humidification- dehumidification system has been theoretically investigated. The newly designed system presented in the current work exhibited a number of attractive attributes that might open new promising opportunities for the advent of freshwater to environments with limited water resources and high solar radiation rates. The effects of feed water flow rate, the inlet water and air temperature and air flow rate on the solar still performance have been considered. Based on the obtained results, the following conclusions can be drawn:

- The Indeed, the productivity of our distiller which using humidification-dehumidification processes (0 to 8.5 kg/m^2) is 63% higher than the productivity of the solar still augmented with a flat-plate collector presented by Badran et al. (2005) (0 to 2.3kg/m^2).
- Decreasing the inlet water temperature to the condenser of solar still leads to increasing the still productivity.
- Increasing the inlet air temperature to the condenser of solar still leads to increase the still productivity.
- For all configurations, modeling of the system and simulating its behavior have been successfully done on the basis of thermal and mass balance approach.
- The effects of incorporating the different modules on the system performance were studied.
- Comparing the obtained results with those of other studies, gives a good validity of the present results.

Acknowledgment

The authors wish to thank the Ministry of Higher Education, Scientific Research and Information and Communication Technologies MESRS-TIC for its financial support to the R&D project entitled “Solar Driven membrane distillation for resource efficient desalination in remote areas”, and the Fraunhofer Institute for Solar Energy Systems ISE for its collaboration.

Nomenclature

Cw : Water heat capacity in the solar water [J/(kg.K)]
Ca : Air heat capacity in the solar still [J/(kg.K)],
Cb : Basin heat capacity [J/(kg.K)],
Cv : Glass cover heat capacity [J/(kg.K)],
Mw : Water mass flow sprayed onto the packed bed [kg/s],
Ma : Air mass flow density in the solar distiller [kg/(m^2.s)],
Mv : Glass cover weight [kg],
Mg : Water weight in the condenser [kg],
Mw : Water weight in the solar distiller [kg],
Mf : Fluid weight in the condenser [kg],
Mab : Absorber weight of solar water [kg],
Ti : Temperature at the air-water interface (packed bed) [°C],
Uloss : Global exchange coefficient between the absorber of the solar distiller and the external environment [W/(m^2 K)],
Wg : Air humidity in the condenser (packed bed) [kg water/kg dry air],
Wa : Air humidity in the solar distiller (packed bed) [kg water/kg dry air],
Wi : Saturation humidity in the solar distiller [kg water/kg dry air],
Uf : Global exchange coefficient of the absorber of the condenser with the outside environment [W/ (m^2 K)],
Uw : Global exchange coefficient of the absorber of the solar water with the outside environment [W/ (m^2 K)],
Tb : Temperature of the absorber Basin distiller [°C],
Ta : Air temperature in the air solar collector [°C],
Tv : Glass cover temperature of the air solar collector [°C],

Tf : Fluid temperature in the condenser tower [°C],
Tic : Air temperature interface in the condenser tower [°C],
Tgc : Air temperature in the condenser tower [°C],
Tg : Glass cover temperature of the solar distiller [°C],
Tamb : Ambient temperature [°C],
Tw : Water temperature in the solar water [°C]
Tve : The input water temperature [°C],
Tpl : Air temperature of absorber plate of air solar collector [°C]
Twe : The input glass cover temperature [°C],
Mem : Energy storage material weight in the solar distiller [kg],
Cem : Energy storage material heat capacity in the solar distiller [J/(kg.K)].
Pw : Vapor pressure at Tw [atm].
Pv : Vapor pressure at Tg[atm].
Um : Mass transfer coefficient of water vapor to the air-water interface [W/(m^2K)].
Uw : Heat exchange coefficient of the water film in the packed bed [W/(m^2K)].
Ua : Heat exchange coefficient of the air film in the packed bed [W/(m^2K)].
Zl : The packed bed height (mm).
Cpw : Water heat transfer coefficient at the air-water interface (W/(m^2.K))
Cpa : Air heat capacity in the packed bed [J/ (kg.K)].
Tl : Temperature at the packed bed [°C].
Aw : Surface of water in the basin of solar still (m^2)
Av : Surface of glass cover (m^2)
Aab : Surface of basin (m^2)
A : Surface (m^2)
Cf : Fluid specific heat (J/(kg.K))
Cpg : Moist air specific heat in the condenser (J/(kg.K))
Cpa : Specific heat (J/(kg.K)) absorber plate mass thermal capacity (J/(kg K))
de : Outer diameter of the condensation tower tube (m)
Hc : Air heat transfer coefficient at the air-water interface in the condenser (W/(m^2.K))
He : Water heat transfer coefficient at the air-water interface in the condenser (W/(m^2.K))
di : Inner diameter of the condensation tower tube (m)
G : G ravitational acceleration (m/s^2)
U : Overall heat transfer coefficient in the condenser (W/ (m^2.K))
Ug : Air film voluminal heat transfer coefficient in the condenser (W/(m^3.K))
Umc : Water vapour voluminal mass transfer coefficient at the vapour-condensate interface in the condensation tower (kg/(m^3.s))
Ua : Air voluminal heat transfer coefficient at the air-water interface in solar still(W/(m^3.K))
Km : Water vapor mass transfer coefficient at the air-water interface (kg/(m^2.s))
L : Tube length of the condensation tower (m)
I : Solar flux (W/m^2)
Mg : Mass velocity of moist air in the condenser (kg/(m.s))
Mw : Water flow rate (kg/s)
Ma : Air flow rate (kg/s)
M : Mass (kg)
Pr : Prandtl number
Re : Reynolds number
P : Pressure (Pa)
Pl : Longitudinal pitch (m)
Pt : Transverse pitch (m)
T : Temperature (K)
Ti : Temperature at the air-water interface (K)
Wic : Saturation humidity in the condenser (kg water/kg dry air)
Wi : Saturation humidity (kg water/kg dry air)
Z : Coordinate in the flow direction (m)
Mem : Energy storage material weight in the solar distiller [kg]
Cem : Energy storage material heat capacity in the solar distiller [J/(kg K)]
Wa : Air humidity (kg water/kg dry air)
Dmc : Water condensation rate (kg/s)
Vwind : Wind velocity (m/s)

Greek

λo : Latent heat of water evaporation (J/kg)
λp : Wall thermal conductivity (W/m K)
λe : Water thermal conductivity (W/m K)
λc : Condensed water thermal conductivity (W/m K)
λgc : Humid air thermal conductivity in the condenser (W/m K)
ρc : Water density (kg/m^3)
μc : Dynamic viscosity of condensed water (Ns/m^2)
μp : Dynamic viscosity at the wall temperature (Ns/m^2)
Σ : Stefan-Boltzman constant
εeff : Effective emissivity
εv : Glass cover emissivity
V : Velocity of fluid (m/s)
αab : Absorbance of the collector absorber surface
T : Transmittance
εw : Water emissivity

Subscripts

A : Moist air in solar still
Amb : Ambient
B : Basin absorber
C : Condenser
F : Feed water
V : Glass cover
W : Water
G : Moist air in condenser
Loss : Loss to ambient

References

[1] L. Chennan, Y. Goswami and E. Stefanakos, Solar assisted sea water desalination: A review, *Renewable and Sustainable Energy Reviews,* 19 (2013) 136-163.

[2] R. Tripathi and G. N. Tiwari, Effect of water depth on internal heat and mass transfer for active solar distillation, *Desalination,* 173 (2) (2005) 187-200.

[3] K. Sampathkumar, T. V. Arjunan, P. Pitchandi and P. Senthilkumar, Active solar distillation- a detailed review, *Renewable and Sustainable Energy* Reviews, 14 (2010) 1503-1526.

[4] K. Schwarzer, E. Vieira da Silva, B. Hoffschmidt and T. Schwarzer, A new solar desalination system with heat recovery for decentralized drinking water production, *Desalination,* 248 (2009) 204-211.

[5] C. Tenthani, A. Madhlopa and C. Z. Kimambo, Improved solar still for water purification, *J. of Sustainable Energy and Environment,* 3 (2012) 111-123.

[6] S. Kumar and A. Tiwari, An experimental study of hybrid photovoltaic thermal (PV/T) active solar still, *Int. J. of Energy Research,* 32 (2008) 847-858.

[7] V. Velmurugan, S. S. Kumaran, V. N. Prabhu and K. Srithar, Productivity enhancement of stepped solar stillperformance analysis, *Thermal Science,* 12 (2008) 153-163.

[8] V. Velmurugan, K. J. Naveen, H. T. Noorul and K. Srithar, Performance analysis in stepped solar still for effluent desalination, *Energy,* 34 (2009) 1179-1186.

[9] A. A. El-Sebaii, A. A. Al-Ghamdi, F. S. Al-Hazmi and A. S. Faidah, Thermal performance of a single basin solar still with PCM as a storage medium, *Applied Energy,* 86 (2009) 1187-1195.

[10] A. M. El-Zahaby, A. E. Kabeel, A. I. Bakry, S. A. El-Agouz and O. M. Hawam, Augmentation of solar still performance using flash evaporation, *Desalination,* 257 (2010) 58-65.

[11] S. Farsad and A. Behzadmehr, Analysis of a solar desalination unit with humidification-dehumidification cycle using DoE method, *Desalination,* 278 (2011) 70-76.

[12] H. Karan Mistry, M. Alexander, H. John and V. Lienhard, Optimal operating conditions and configurations for humidification-dehumidification desalination cycles, *Int. J. of Thermal Sciences,* 50 (2011) 779-789.

[13] K. Ronan et al., Performance limits of zero and single extraction humidification dehumidification desalination systems, *Applied Energy,* 102 (2013) 1081-1090.

[14] J. H. Juan, A. Camilo and A. E. Claudio, Water desalination by air humidification: Mathematical model and experimental study, *Solar Energy,* 86 (2012) 1070-1076.

[15] M. Morteza and A. Majid, Constructional design and optimization of a direct contact humidification- dehumidification desalination unit, *Desalination,* 293 (2012) 69-77.

[16] H. Ben Bacha and K. Zhani, Contributing to the improvement of the production of solar still, *Desalin. Water Treat*., 51 (4-6) (2013) 1310-1318.

[17] K. Zarzoum, K. Zhani and H. Ben Bacha, Improving the design, modeling and simulation in dynamic mode of a solar still, *International Journal of Desalination and Water Treatment*, DOI:10.1080/19443994.2013.821031 (2013).

[18] K. Zhani, H. Ben Bacha and T. Damak, A study of a water desalination unit using solar energy, *Desalination and Water Treatment,* 3 (2009) 261-270.

[19] K. Zhani and H. Ben Bacha, Modeling and simulation of a new design of the SMCEC desalination unit using solar energy, *Desalination and Water Treatment,* 21 (2010) 346-356.

[20] K. Zhani and H. Ben Bacha, An approach to optimize the production of solar desalination unit using the SMCEC principle, *Desalination and Water Treatment,* 13 (2010) 96-107.

[21] M. B. Amara, I. Houcine, A. A. Guizani and M. Mâalej, Theoretical and experimental study of a pad humidifier used on an operating seawater desalination process, *Desalination*, 168 (2004) 1-12.

[22] *Fundamental handbook Tome,* Ashrae (1977).

[23] W. F. Stoecker and J. W. Jones, *Refrigeration and air conditioning*, 2nd ed., New York: McGraw Hill (1982).

[24] A. S. Nafey, H. E. S. Fath, S. O. El-Helaby and A. M. Soliman, Solar desalination using humidification dehumidification processes, Part I. A numerical investigation, *Energy Conv. Mgmt*., 45 (7-8) (2004) 1243-1261.

[25] T. Damak, Modelisation, estimation et commande de procedes biotechnologiques de type hyperbolique, *Ph.D. Thesis*, Universite Paul Sabatier, Toulouse, France (1994).

[26] R. K. Srivastava and B. Joseph, Reduced-order model for separation columns, V. Selection of collocation points, *Comput. Chem. Eng.* (1985) 9:601e13.

[27] A. B. Akash, S. M. Mohsen, O. Omar and E. Yaser, Experimental evaluation of a single- basin solar still using different absorbing materials, *Renewable Energy* (1998) 307-310.

[28] K. K. Murugavela, S. Sivakumara, J. R. Ahameda, K. K. S. K. Chockalingama and K. Sritharb, Single basin double slope solar still with minimum basin depth and energy storing materials, *Energy* (2010) 514-523.

K. Zarzoum is a Ph.D. Student at National Engineering School at Sfax (ENIS), University of Sfax, Tunisia. His research interests include Desalination Renewable Energy (Solar energy application for water desalination.

K. Zhani is an Assistant Professor in the mechanical department at the higher Institute of Applied Sciences and Technology of Kairouan (ISSATK), University of Kairouan - Tunisia. He holds a Ph.D. in mechanics (ENIS, University of Sfax, April 2011).

H. Ben Bacha is a Full Professor at Engineering School of Sfax (Ecole Nationale d'Ingénieurs de Sfax - ENIS), University of Sfax – Tunisia and a Manager of training at the ENIS since 2005. And he is also a head of Team Renewable Energy at the Laboratoire des Systèmes Electromécaniques (LASEM). His research fields are water desalination by solar energy, air conditioning by solar energy and maintenance of systems.